Journal of Alloys and Compounds 509 (2011) 5269–5273

Contents lists available at ScienceDirect

Journal of Alloys and Compounds

journal homepage: www.elsevier.com/locate/jallcom

Experimental phase diagram of the Ti–Si–Sn ternary system at 473 K

Yongzhong Zhan[a,b,*], Wenchao Yang[a], Yanfei Xu[a], Xinjiang Zhang[a]

[a] Laboratory of Nonferrous Metal Materials and New Processing Technology, Ministry of Education, Guangxi University, Nanning, Guangxi 530004, PR China
[b] International Center for Materials Physics, Chinese Academy of Sciences, Shenyang 10016, PR China

ARTICLE INFO

Article history:
Received 6 May 2010
Received in revised form 10 February 2011
Accepted 11 February 2011
Available online 21 February 2011

Keywords:
Metals and alloys
Phase diagrams
X-ray diffraction
Scanning electron microscopy
SEM

ABSTRACT

The phase diagram of the ternary system Ti–Si–Sn system at 473 K was investigated by means of powder X-ray diffraction (XRD), differential thermal analysis (DTA) and scanning electron microscope (SEM) with energy dispersive analysis (EDX). The isothermal section consists of 14 single phase regions, 26 binary phase regions and 13 ternary phase regions. The 10 binary compounds, namely Ti_3Si, Ti_5Si_3, Ti_5Si_4, TiSi, $TiSi_2$, Ti_3Sn, Ti_2Sn, Ti_5Sn_3, Ti_6Sn_5, Ti_2Sn_3, have been confirmed at 473 K. Moreover, a ternary phase with the crystal structure of tetragonal W_5Si_3 structure type and I4/mcm space group is confirmed in the Ti–Si–Sn system. The combined results of both EDX and XRD show that the composition of this ternary phase is 60.25–61.03 at.% Ti, 15.01–21.77 at.% Si and balance Sn.

1. Introduction

Titanium and its alloys as important structural materials are widely used in many fields such as aerospace, automobile, and medical appliances, due to their low density, high specific strength and modulus, and corrosion resistance. As a new titanium-casting alloy, the Ti–Si eutectic alloy has a strengthening mechanism that greatly differs from the traditional titanium alloys. Si is important constituent of multicomponent Ti-alloys [1,2], because it can essentially increase the corrosion and creep resistance and high-temperature strength of both titanium and Ti–Al alloys. As a conventional alloying addition for Ti alloys, Sn can improve the quenchability and viscosity of β-Ti [3]. Despite this, multicomponent phase diagrams on the basis of Ti, Si and Sn are mostly unknown. Moreover, phase equilibria in the boundary Ti–Si–Sn ternary were reported only in Refs. [4,5], however, in a narrow concentration interval. Therefore, it is essential to investigate further the phase relationship of the Ti–Si–Sn ternary system for developing polynary cast titanium alloys with high performance.

According to Ref. [6], five compounds, i.e. Ti_3Si, Ti_5Si_3, Ti_5Si_4, TiSi and $TiSi_2$, were found in the Ti–Si binary system. In Ref. [7], the Si–Sn phase diagram was reported without compounds. The Ti–Sn binary phase diagram [8] shows four intermediate phases of Ti_3Sn, Ti_2Sn, Ti_5Sn_3 and Ti_6Sn_5. Yet, a new phase Ti_2Sn_3 has been confirmed in the isothermal section of the ternary La–Ti–Sn and Cu–Ti–Sn systems at 473 K [9,10]. This binary compound was revealed for the first time by Kuper et al. [11] and its crystal has been identified by Künnen et al. [12]. Structural data for the intermetallic compounds in the three binary systems are given in Table 1.

The purpose of the present work is to investigate experimentally the Ti–Si–Sn phase diagram, mainly by assemble an isothermal section at 473 K, so as to provide essential information for the design and fabrication of new-type titanium alloys with high performance.

2. Experimental details

The present investigation was carried out with 100 samples having weight of 2 g. The purities of the starting materials, namely, titanium, silicon and tin were 99.8 wt.%, 99.99 wt.% and 99.99 wt.%, respectively. The alloy buttons were produced by arc melting on a water-cooled copper crucible with a non-consumable tungsten electrode under pure argon atmosphere. Each as-arc-cast button was melted three times and turned around after melting for better homogeneity. Since the alloys contain tin, the electric current was as low as possible so as to minimize the weight loss by volatilization of tin. For most alloys, the weight loss was less than 1% after melting.

The as-cast samples were sealed in an evacuated quartz tube for homogenization treatment and then annealed at different temperatures in order to attain good homogenization. The heat treatment temperature was determined on the basis of the binary alloy phase diagrams of the Ti–Si, Ti–Sn and Si–Sn systems [8–10] and the results of differential thermal analysis (DTA) of some typical samples. The binary samples that contain more than 75% Sn in the Si–Sn system or 45.5% Sn in the Ti–Sn system, as well as the ternary samples with Sn content higher than 60%, were initially annealed at 773 K for 720 h and then cooled down to 473 K at a rate of 0.15 K/min, then kept at 473 K for 240 h. Other samples were homogenised initially at 1073 K for 720 h, then cooled down to 473 K at a rate of 0.15 K/min, and finally kept at 473 K for 240 h. Finally, all these annealed buttons were quenched in liquid nitrogen.

X-ray powder diffraction (XRD) and scanning electron microscopy (SEM) with energy dispersive analysis (EDX) were used in the present investigation. Samples for

* Corresponding author at: Institute of Materials Science, School of Physics, Daxue Road, 100 Nanning, Guangxi 530004, China. Tel.: +86 771 3272311; fax: +86 771 3233530.
E-mail address: zyzmatres@yahoo.com.cn (Y. Zhan).

0925-8388/$ – see front matter © 2011 Elsevier B.V. All rights reserved.
doi:10.1016/j.jallcom.2011.02.062

Table 1
Binary crystal structure data in the Ti–Si–Sn system.

Compound	Space group	Lattice parameters (nm)			Reference
		a	*b*	*c*	
Ti_3Si	$P4_2/n$	1.0196	–	0.5097	[13]
Ti_5Si_3	$P6_3/mcm$	0.7461	–	0.5151	[13]
Ti_5Si_4	$P4_12_12$	0.7133	–	1.2977	[13]
TiSi	Pnma	0.657	0.364	0.503	[13]
$TiSi_2$	Fddd	0.8036(6)	0.4773(4)	0.8523(6)	[13]
Ti_3Sn	$P6_3/mmc$	0.5916	–	0.4764	[14]
Ti_2Sn	$P6_3/mmc$	0.4653	–	0.569	[14]
Ti_5Sn_3	$P6_3/mcm$	0.8049(2)	–	0.5454(2)	[14]
Ti_6Sn_5	$P6_3/mmc$	0.922	–	0.569	[14]
Ti_2Sn_3	Cmca	0.596	1.994	0.702	[12]

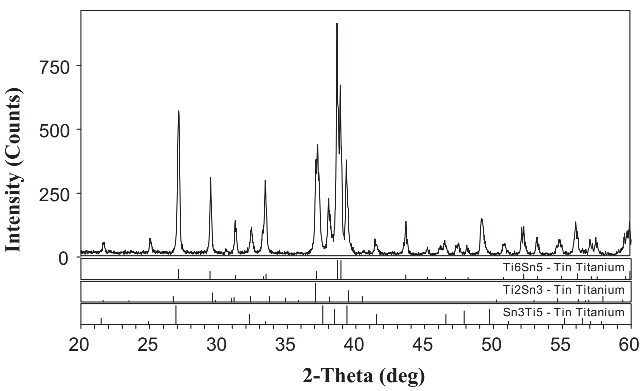

Fig. 1. The XRD pattern of the sample with 54 at.% Ti, 6 at.% Si and 40 at.% Sn containing Ti_2Sn_3, Ti_6Sn_5 and Ti_5Sn_3.

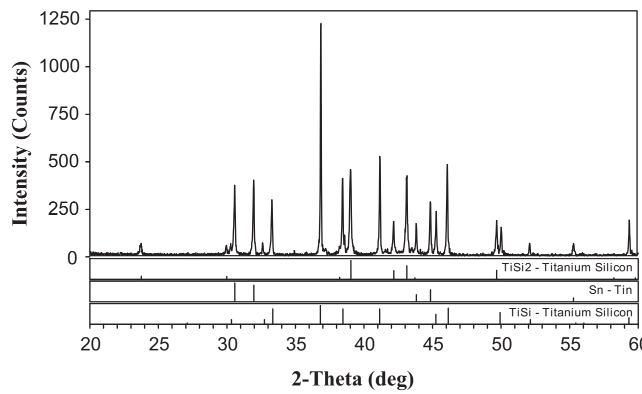

Fig. 3. The XRD pattern of the sample with 30 at.% Ti, 40 at.% Si and 30 at.% Sn containing $TiSi_2$, TiSi and Sn.

XRD analysis were initially powdered and then measured with the help of Rigaku D/Max 2500 V diffractometer with Cu Kα radiation and graphite monochromator operated at 40 kV, 200 mA. The Materials Data Inc. software Jade 5.0 [15] and powder diffraction file (PDF release 2002) were used for phase identification. By all these means, the phases relation and the crystal structure of the Ti–Si–Sn ternary system were determined.

3. Results and discussions

3.1. Boundary binary systems

At 473 K, the binary compounds in the Ti–Si, Ti–Sn and Si–Sn binary systems have been confirmed. In the Ti–Sn system, a new stable phase Ti_2Sn_3 has been confirmed in the isothermal section of the ternary La–Ti–Sn and Cu–Ti–Sn systems at 473 K in the authors' previous publications [9,10]. In the present work, the XRD pattern of the equilibrated sample with (54 at.% Ti, 6 at.% Si and 40 at.% Sn) composition also clearly indicates the existence of Ti_2Sn_3 besides Ti_6Sn_5 and Ti_5Sn_3 phases, as illustrated in Fig. 1. In addition, the XRD pattern of the equilibrated sample with 50 at.% Ti, 10 at.% Si and 40 at.% Sn clearly indicates the existence of three phases namely Ti_2Sn_3, Sn and Ti_5Sn_3 in Fig. 2. Based on this experimental result, five binary compounds Ti_3Sn, Ti_2Sn, Ti_5Sn_3, Ti_6Sn_5 and Ti_2Sn_3 have been observed in Ti–Sn system.

In the Ti–Si system, five phases i.e. Ti_3Si, Ti_5Si_3, Ti_5Si_4, TiSi and $TiSi_2$ have been confirmed. It agrees well with the results of Ref. [13]. For example, Fig. 3 illustrates the XRD pattern of the equilibrated sample (30 at.% Ti, 40 at.% Si and 30 at.% Sn) containing three phases of $TiSi_2$, TiSi and Sn, which clearly proves that the $TiSi_2$ and TiSi binary compounds exist in the present isothermal section.

According to the present work, no binary compound exists in the Si–Sn system, which is confirmed by the XRD results of some

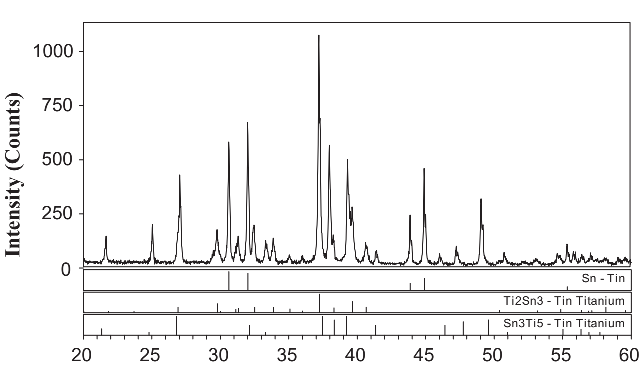

Fig. 2. The XRD pattern of the sample with 50 at.% Ti, 10 at.% Si and 40 at.% Sn containing Ti_2Sn_3, Sn and Ti_5Sn_3.

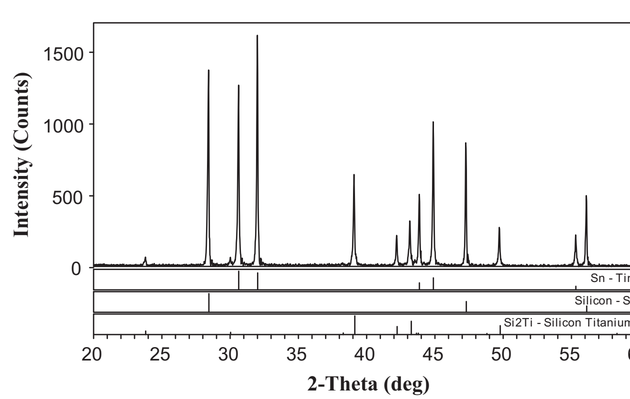

Fig. 4. The XRD pattern of the sample with 10 at.% Ti, 60 at.% Si and 30 at.% Sn containing Sn, Si and $TiSi_2$.

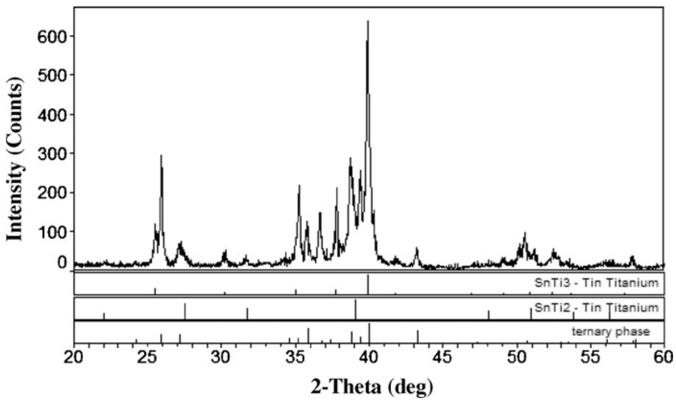

Fig. 5. The XRD pattern of the Ti68Si6Sn26 sample (68 at.% Ti, 6 at.% Si and 26 at.% Sn) containing Ti_2Sn, Ti_3Sn and the ternary phase.

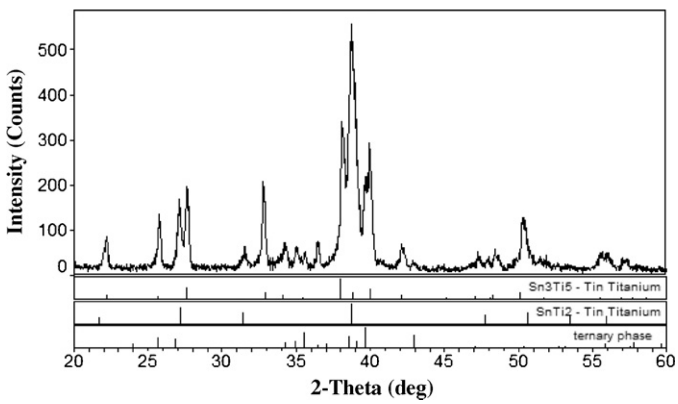

Fig. 6. The XRD pattern of the Ti64Si6Sn30 sample (64 at.% Ti, 6 at.% Si and 30 at.% Sn) containing Ti_5Sn_3, Ti_2Sn and the ternary phase.

binary alloys on this boundary system and the equilibrated sample with 10 at.% Ti, 60 at.% Si and 30 at.% Sn which contains $TiSi_2$, TiSi and Sn phases (Fig. 4).

3.2. The new ternary compound

While analyzing the results of the XRD patterns of the equilibrated samples in the Ti-rich region of 60–75 at.%, the existence of a ternary compound was always clearly observed. For example, the XRD pattern of the equilibrated sample containing 68 at.% Ti, 6 at.% Si and 26 at.% Sn clearly indicates the existence of Ti_2Sn and Ti_3Sn phases besides the ternary compound, as illustrated in Fig. 5. Moreover, Fig. 6 shows that the XRD pattern of the sample with 64 at.% Ti, 6 at.% Si and 30 at.% Sn contains Ti_5Sn_3, Ti_2Sn and the ternary phase. In addition, the XRD pattern of the equilibrated Ti60Si23Sn17 sample (60 at.% Ti, 23 at.% Si and 17 at.% Sn) and Ti66Si16Sn18 sample (66 at.% Ti, 16 at.% Si and 18 at.% Sn) also clearly indicates the existence of this ternary compound. It is shown in Figs. 7 and 8 that the Ti60Si23Sn17 sample contains Ti_5Si_3, Ti_5Sn_3 and the ternary

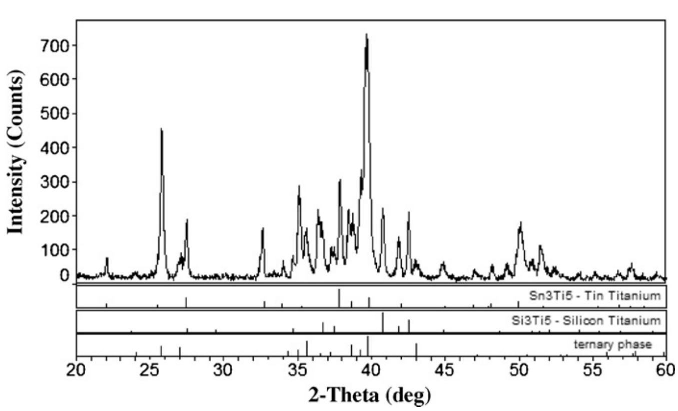

Fig. 7. The XRD pattern of the Ti60Si23Sn17 sample (60 at.% Ti, 23 at.% Si and 17 at.% Sn) containing Ti_5Sn_3, Ti_5Si_3 and the ternary phase.

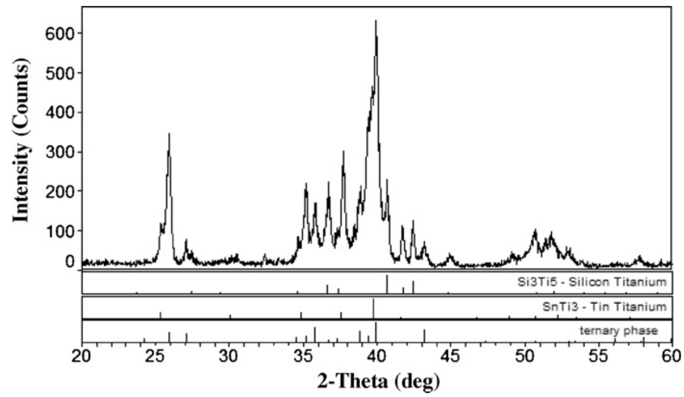

Fig. 8. The XRD pattern of the Ti66Si16Sn18 sample (66 at.% Ti, 16 at.% Si and 18 at.% Sn) containing Ti_5Si_3, Ti_3Sn and the ternary phase.

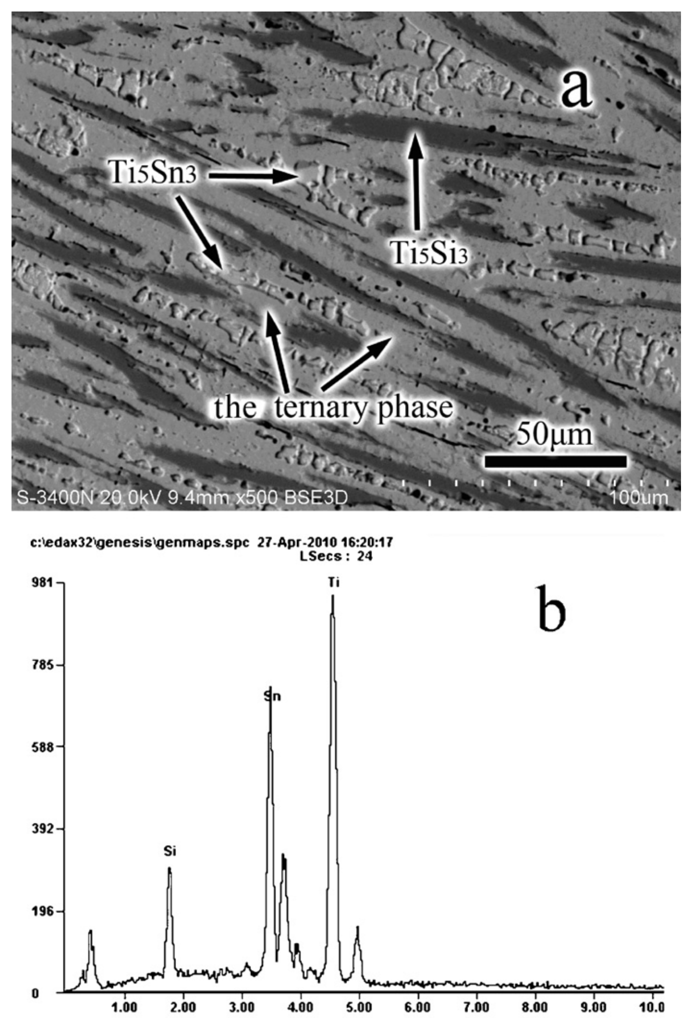

Fig. 9. The microstructure of the equilibrated Ti60Si23Sn17 sample (a) and EDX result of the ternary phase (b).

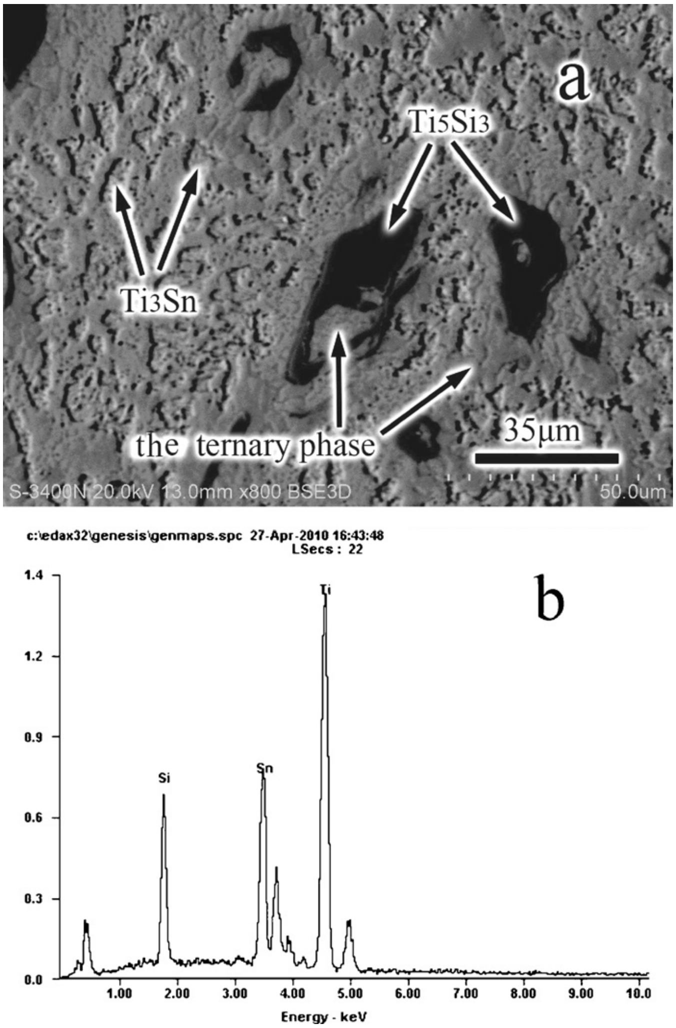

Fig. 10. The microstructure of the equilibrated Ti66Si16Sn18 sample (a) and EDX result of the ternary phase (b).

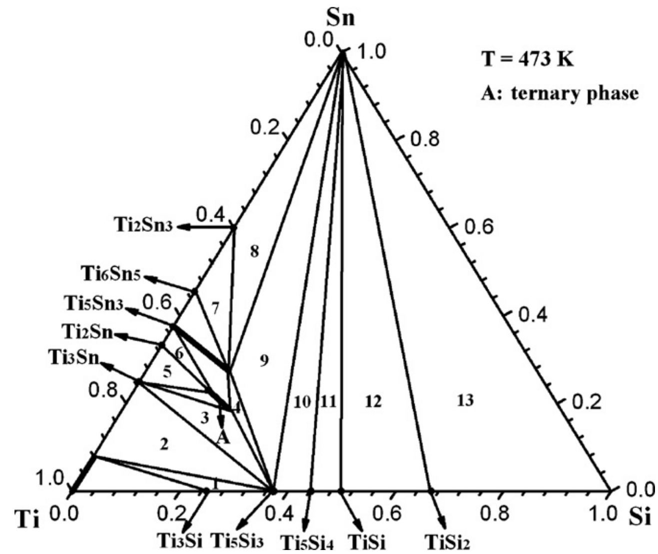

Fig. 11. The isothermal section of the Ti–Si–Sn ternary system at 473 K.

Table 2
Details of the three-phase regions in the Ti–Si–Sn at 473 K.

Phase regions	Alloy composition (at.%)			Phase composition
	Ti	Si	Sn	
1	74	24	2	$Ti + Ti_3Si + Ti_5Si_3$
2	76	8	16	$Ti + Ti_3Sn + Ti_5Si_3$
3	66	16	18	$Ti_3Sn + Ti_5Si_3$ + ternary phase
4	60	23	17	$Ti_5Sn_3 + Ti_5Si_3$ + ternary phase
5	68	6	26	$Ti_3Sn + Ti_2Sn$ + ternary phase
6	64	6	30	$Ti_2Sn + Ti_5Sn_3$ + ternary phase
7	56	4	40	$Ti_6Sn_5 + Ti_5Sn_3 + Ti_2Sn_3$
8	50	10	40	$Ti_5Sn_3 + Ti_2Sn_3 + Sn$
9	50	20	30	$Ti_5Sn_3 + Ti_5Si_3 + Sn$
10	42	28	30	$Ti_5Si_3 + Sn + Ti_5Si_4$
11	32	28	40	$Ti_5Si_4 + TiSi + Sn$
12	30	40	30	$TiSi + TiSi_2 + Sn$
13	10	60	30	$TiSi_2 + Si + Sn$

phase, and the Ti66Si16Sn18 sample consists of Ti_5Si_3, Ti_3Sn and the ternary phase, respectively. The crystal structure of the ternary compound was shown to be tetragonal W_5Si_3 structure type and I4/mcm space group. The microstructures of the Ti60Si23Sn17 and Ti66Si16Sn18 samples examined by SEM and EDX clearly indicated the existence of three phases, as is shown in Figs. 9a and 10a, respectively. According to Ref. [5], Bulanova et al. have reported that the ternary compound of composition $Ti_5Si_{1.2–1.6}Sn_{1.8–1.4}$ was found in the Ti–Si–Sn alloys. The Ti concentration is stable at 62.5 at.%, Si content is 15–20 at.%, and the surplus is Sn content. However, in this work, based on the EDX result of the ternary phase in the Ti60Si23Sn17 (Fig. 9b) and Ti66Si16Sn18 (Fig. 10b) samples, Ti and Si contents are determined to be 60.25–61.03 at.%, 15.01–21.77 at.%, and the surplus is Sn content. The composition of this ternary phase is basically consistent with the result reported by Bulanova et al. This ternary phase has a rather wide homogeneity range because of the mutual substitution of Si and Sn atoms.

3.3. Isothermal section of the Ti–Si–Sn system at 473 K

The isothermal section of the Ti–Si–Sn system phase diagram at 473 K has been constructed by using the analysis results obtained in the present work, as shown in Fig. 11. This isothermal section consists of 13 three-phase regions, 26 two-phase regions and 14 single-phase regions in this ternary system at 473 K. The solid solubility ranges of all single phases in this isothermal section were determined by using the phase-disappearing method and comparing the shift of the XRD patterns of the samples near the compositions of the phase. At 473 K, the solubility of Si in Ti_5Sn_3 is about 15 at.%, and the solubility of Sn in Ti is about 8 at.%. Details of the 13 three-phase regions are given in Table 2.

4. Conclusions

The phase relationships of the Ti–Si–Sn ternary system at 473 K have been determined. The isothermal section consists of 14 single phase regions, 26 binary phase regions and 13 ternary phase regions. At 473 K, 10 binary compounds in the Ti–Si–Sn system have been confirmed, namely Ti_3Si, Ti_5Si_3, Ti_5Si_4, TiSi, $TiSi_2$, Ti_3Sn, Ti_2Sn, Ti_5Sn_3, Ti_6Sn_5, Ti_2Sn_3. Furthermore, a ternary phase with the crystal structure of tetragonal W_5Si_3 structure type and I4/mcm space group is confirmed for the Ti-rich region of 60.25–61.03 at.% Ti, 15.01–21.77 at.% Si, and balance Sn.

Acknowledgements

This work was jointly supported by the National Natural Science Foundation of China (50761003) and the opening project of State Key Laboratory of Metastable Materials Science and Technology (201005).

References

[1] Y. Du, C. He, J.C. Schuster, S. Liu, H.H. Xu, Int. J. Mater. Res. 97 (2006) 543–555.
[2] H. Xu, Y. Du, H. Chen, Y. He, Z. Pan, J.C. Schuster, R. Wang, J. Alloys Compd. 394 (2005) 235–239.
[3] A.A. Popov, L.I. Anisimova, Metallovedeniye itermicheskaya obrabotka 12 (1985) 45–50, in Russian.
[4] M. Bulanova, A. Soroka, P. Zheltov, V. Vereshchaka, K. Meleshevich, Z. Metallkd. 90 (1999) 505–507.
[5] M. Bulanova, L. Tretyachenko, K. Meleshevich, V. Saltykov, V. Vereshchaka, O. Galadzhyj, L. Kulak, S. Firstov, J. Alloys Compd. 350 (2003) 164–173.
[6] J.L. Murray, Binary Alloy Phase Diagrams, ASM International, Materials Park, OH, 1987.
[7] R.W. Olesinski, G.J. Abbaschian, Binary Alloy Phase Diagrams, ASM International, Materials Park, OH, 1984.
[8] P. Pietrokowsky, E.P. Frink, Trans. ASM 49 (1957) 339–342.
[9] Y. Zhan, Y. Xu, H. Xie, Z. Yu, Y. Wang, Y. Zhuang, J. Alloys Compd. 459 (2008) 174–176.
[10] X. Zhang, Y. Zhan, Q. Guo, G. Zhang, J. Hu, J. Alloys Compd. 480 (2009) 382–385.
[11] C. Kuper, W. Peng, A. Pisch, F. Goesmann, R. Schmid-Fetzer, Z. Metallkd. 89 (1998) 855–862.
[12] B. Künnen, W. Jeitscko, G. Kotzuba, B.D. Mosel, Z. Naturforsch. 55b (2000) 425–439.
[13] P. Villars, Pearson's Handbook of Crystallographic Data, ASM International, Materials Park, OH, 1997, pp. 2842–2843.
[14] P. Villars, Pearson's Handbook of Crystallographic Data, ASM International, Materials Park, OH, 1997, p. 2255.
[15] Jade 5.0, XRD Pattern Processing Materials Data Inc., 1999.